AIAA JOURNAL
Vol. 30, No. 10, October 1992

Analysis of the Onset of Dynamic Stall

Jeffrey M. Currier* and K.-Y. Fung†
University of Arizona, Tucson, Arizona 85721

The dynamic stall characteristics of several airfoils have been investigated to assess the effects of compressibility, unsteadiness, and airfoil geometry on the onset of dynamic stall. For the purpose of understanding the physical phenomena in the range of low reduced frequency of practical importance, it is found that the flow before the onset of stall can be considered quasisteady and hence predicted using inviscid theory. For moderate Reynolds number, our analysis predicts the presence of a separation bubble at the airfoil leading edge and suggests that bubble bursting, or failure to reattach after the initial separation, is the onset mechanism. It is found in numerical simulation that at angles of attack close to static stall minor movements in transition point location can cause bursting of the separation bubble and that bursting is more susceptible to transition location in a locally supersonic flow than in subsonic flow. Finally, it is found that the delay between passage through the static stall angle and the onset of dynamic stall decreases with increasing unsteadiness. This result suggests that separation is being promoted rather than delayed and that the lift benefits from dynamic stall only for the duration of the separation process.

Nomenclature

A = pitch rate per unit dimensionless time, deg
C = airfoil chord
C_ℓ = lift coefficient
C_{ℓ_α} = lift curve slope
C_p = wall static-pressure coefficient, $(P - P_\infty)/(\rho U_\infty^2/2)$
C_{p_m} = maximum suction peak, minimum pressure coefficient
K = Reynolds number ratio at separation, $R_{\delta_s}/\sqrt{R}$
k = reduced frequency, $\omega C/(2U_\infty)$
M = Mach number
R, Re = Reynolds number
S' = coordinate along airfoil contour from stagnation point
t = dimensionless time based on half chord traveled
U = flow speed
u, v = velocity components
α = angle of attack, deg
δ = displacement thickness
θ = momentum thickness
Λ = Gaster's bubble parameter, $(\theta_s^2/\nu)(\Delta U/\Delta S)$
ν = kinematic viscosity
σ = $(p_{\text{at reattachment}} - p_s)/(\rho u_s^2/2)$

Subscripts

e = just outside the boundary layer
s = value at laminar separation point
0 = value at stagnation point
∞ = freestream value

Introduction

RAPID upward pitching of the airfoil is an important consideration for the design of helicopter rotor blades. Once the angle of attack α exceeds a critical value, a vortex separates from the leading edge. The low suction pressure associated with this separation vortex increases lift dramatically until the vortex leaves the trailing edge. It is commonly believed that this unsteady upward pitching motion of the airfoil has a favorable effect on delaying boundary-layer separation and hence increases the lift for α beyond the static stall angle. This process of creating lift beyond the static stall lift limit has become known as dynamic stall.

In the absence of dynamic effects, the flow over an airfoil must be massively separated for α in excess of the static stall angle. For dynamic stall, however, the separation process depends on the nature of the flow before stall. According to McCullough and Gault,[1] there are three types of static stall: trailing-edge stall, thin-airfoil stall, and leading-edge stall. Trailing-edge stall is characterized by the forward movement of the turbulent separation point from the trailing edge. Thin-airfoil stall is preceded by laminar flow separation at the leading edge with laminar or turbulent reattachment at a point downstream that moves rearward with increasing α. The body streamline that bifurcates at the separation point and merges at the reattachment point encompasses a region commonly referred to as a long separation bubble, since its length can be comparable to the chord. Leading-edge stall is also preceded by laminar flow separation near the leading edge that almost immediately reattaches because of rapid transition to turbulent flow. The size of the region between separation and reattachment is comparable to the thickness of the boundary layer and becomes shorter as the stall angle is approached. At stall, immediate reattachment is no longer possible, resulting in massive separation of the boundary layer, or bursting of the separation bubble. However, if conditions allow, the separated flow may reattach, directing the outward vortical flow back to the body surface to form a long bubble. The drastic loss of lift commonly referred to as stall is experienced only when the separated flow fails to reattach.

The onset of stall for a pitching airfoil may be delayed to a much higher angle than the static stall value or in some cases may be totally prevented. Ham and Garelick[2] observed that this extra lift could be explained if on the retreating blade (moving in the direction opposite to flight) the lift, enhanced by equivalent rapid pitching motions, is greater than the lift predicted by steady flow theory. Harper and Flanigan[3] showed that, if an aircraft is rapidly pitched, the lift can be significantly increased. Johnson and Ham[4] showed that the delay of stall for a 12% Joukowsky airfoil is proportional to the nondimensional pitch rate and attributed this delay in bursting of the separation bubble to a lag in the forward movement of the reattached portion of the separation bubble as α is increased. Ericsson and Reding[5] reviewed the various delay mechanisms

Received Oct. 5, 1990; presented as Paper 91-0003 at the AIAA 29th Aerospace Sciences Meeting, Reno, NV, Jan. 7-10, 1991; revision received March 10, 1992; accepted for publication March 15, 1992.

*Graduate Student; currently, Member of Technical Staff, McDonnell Douglas Helicopter Company, Mesa, AZ 85205. Member AIAA.
†Associate Professor, Department of Aerospace and Mechanical Engineering. Member AIAA.

found in a wide range of dynamic stall experiments and presented heuristic models for their prediction.

In the present work, we study the onset of stall for airfoils undergoing oscillatory and ramp-type motions about the static stall angle. We characterize the boundary layer before the onset of separation or the formation of the dynamic stall vortex. Selected data sets from the experiments of McCroskey et al.[6] and Lorber and Carta[7] were examined to characterize the dependence of the onset on parameters thought to be pertinent. Computed pressure distributions were obtained to represent the condition of the outer flow before the onset of stall and used to estimate the condition of the separating boundary layer. It is found that, as α increases, the separation bubble becomes increasingly susceptible to breakdown, especially when the local flow becomes supersonic. A numerical study was conducted to assess the sensitivity of the separating boundary layer to the transition location, simulated by changing the switch-on location of the turbulence model. Again, as α approaches the static stall value, the flow is increasingly sensitive to the transition location, especially when it is locally supersonic.

Experimental Data Sets

To study the onset mechanism of dynamic stall, two experimental data sets were examined. The first was obtained at NASA-Ames Research Center by McCroskey et al.[6] This data set includes experiments on eight airfoils: NACA 0012, Ames A-01, Wortmann FX-098, Sikorsky SC-1095, Hughes HH-02, Vertol VR-7, NLR-1, and NLR-7301. For each of these eight airfoils, pressure histories phase averaged over 50 cycles were

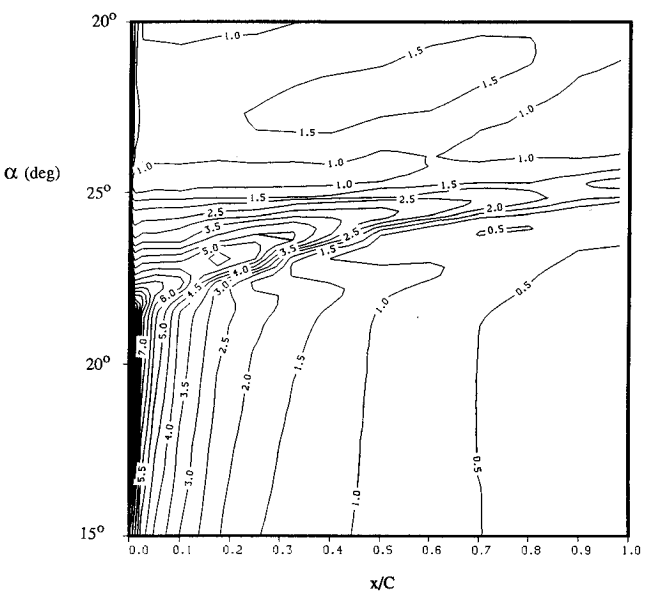

Fig. 1 Pressure coefficient contours for Ames-01 at $M_\infty = 0.184$ and $k = 0.148$.

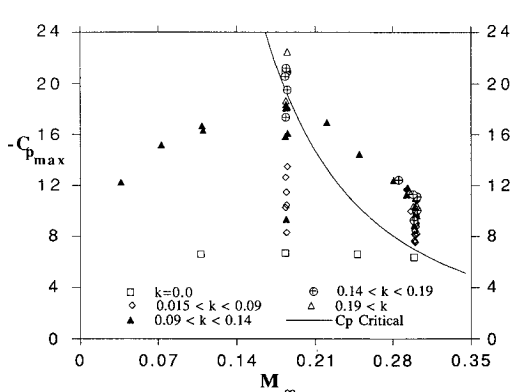

Fig. 2 Maximum suction peak limit for VR-7 airfoil.

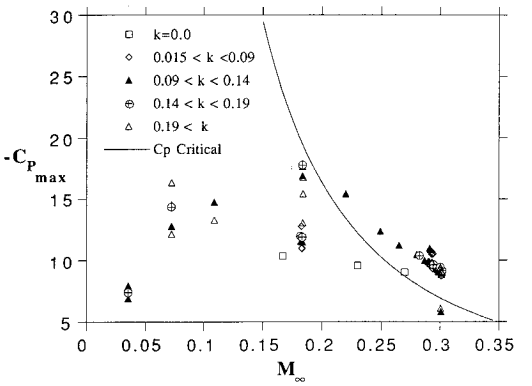

Fig. 3 Maximum suction peak limit for NACA 0012 airfoil.

recorded for sinusoidal pitch oscillations. These oscillations varied in mean angle, amplitude, and frequency. The freestream Mach number M_∞ ranged from 0.035 to 0.302 and the chord Reynolds number Re from 4.9×10^5 to 3.9×10^6. The McCroskey data comprise 1226 cases with an average of 153 cases per airfoil.

The second set of data was obtained at United Technologies Research Center by Lorber and Carta.[7] The set consists of data for a Sikorsky SSC-A09 airfoil section undergoing sinusoidal pitch oscillations and constant-rate pitch ramps. Lorber and Carta used 18 primary pressure transducer locations and took 1000 time samples. The advantage of this data set is that it has five times as many time steps per case as the McCroskey data. On the other hand, there are only 19 cases compared with the 1226 cases in the McCroskey data.

Suction Peak Analysis

The dynamic stall data of McCroskey et al.[6] were examined using computer graphics to visualize the pressure variations in space and time. Figure 1 shows a typical pressure coefficient contour plot. The ordinate is the instantaneous incidence angle of the airfoil and the abscissa is chord location. A very distinct feature, corresponding to shedding of the dynamic vortex from the leading edge, is immediately evident for all cases with stalls initiating during the upward stroke. This feature, seen as spillage of low-pressure contours (with higher contour values corresponding to lower pressures), originates within 2% of the leading edge and is convected at roughly one-third the freestream speed. Before the spillage, the contours are smooth, steeper toward the leading edge, and steeper as α increases, suggesting that pressure is largely unaffected by the boundary layer. This spillage causes the pressure contours to form a suction peak. In some cases, a second similar but much weaker feature can be found at about the same time (angle) some distance downstream of the first. The second feature, seen here at 22 deg and 20% chord, seemingly unconnected to the first, appears to be a separation vortex triggered by the onset of the first. From the more than 75 plots examined, it can be concluded that the onset of stall originates within 2% of the leading edge and is preceded by an absolute minimum of the pressure.

The maximum peak suction has been used to signal abrupt changes in the flow. Rhode[8] in his 1944 wartime report reported an apparent limit, which decreases with M_∞, on all of the suction values recorded during various flight maneuver tests for several airplanes. Johnson and Ham[4] used the loss of suction at a location on the airfoil to indicate dynamic stall. Fung and Carr[9] pointed out that the peak suction values recorded for all of the dynamic stall tests on the NACA 0012 at $M_\infty = 0.3$ were roughly the same, whereas those for lower Mach numbers varied with frequency, amplitude, and mean angle of oscillation. This observation led them to conjecture that the onset of stall for Mach-supercritical flow is shock related, despite the fact that no shock was evident in the experiments.

We have conducted a study similar to that of Fung and Carr[9] using a much larger set of data. Figure 2 shows the dependence of the maximum suction peak on M_∞ (or Re) for all of the dynamic stall experiments on the VR-7.[6] The solid curve shows the critical C_p at which the local flow speed is equal to the speed of sound. The squares represent suction peaks for static stall cases, and other symbols represent maximum suction peaks for different reduced frequency ranges. For values below the critical C_p line, a general trend can be observed that the suction peak overshoot above the static stall value increases with increasing frequency. However, values above the critical C_p become almost insensitive to the pitching frequency. Hence, the lift is less sensitive to changes in frequency at higher Mach numbers and the dynamic effect on the delay of stall onset vanishes. This insensitivity to pitching frequency, amplitude, and mean angle was pointed out by Fung and Carr.[9] Figure 3 shows the same relationship for the NACA 0012 airfoil. Here the overshoots are less pronounced and sensitive to frequency than those of the VR-7, and except for a few cases in which the flow is fully attached throughout the oscillation cycle, all maximum peak suction values for nonzero pitching frequencies are at or above the static values. It is interesting to note that the static stall suction values for all of the airfoils of Ref. 6, except the NACA 0012 and HH-02, stay about the same (see, for example, the squares in Fig. 2), suggesting that the static stalls are of the same type for the range of Reynolds numbers of the experiment. For the NACA 0012 and the lowest Reynolds number tested, $Re = 4.9 \times 10^5$ ($M_\infty = 0.035$), the peak suction values are substantially lower than those at higher Reynolds (Mach) number (Fig. 3). A close look at the pressure contours (a typical one is shown in Fig. 4) of all cases for this airfoil at this Reynolds number revealed that a pressure plateau of about 2% chord followed by a steep pressure recovery appears at the leading edge once α exceeds 12 deg regardless of whether stall is static or dynamic. For these cases, the existence of a separation bubble before stall is clear, and its bursting is likely to be the mechanism for the onset of static or dynamic stall. For all higher Reynolds (Mach) numbers, the existence of a bubble is not readily discernible from the pressure contours. Even for a different pitching scheme, different airfoil, and wider Mach number range (up to $M_\infty = 0.4$), suction peak values taken from the Lorber and Carta[7] data set behave very much the same as those shown in Figs. 2 and 3, and the same phenomenon that led Fung and Carr[9] to suggest that shocks are involved in the onset of separation exists.

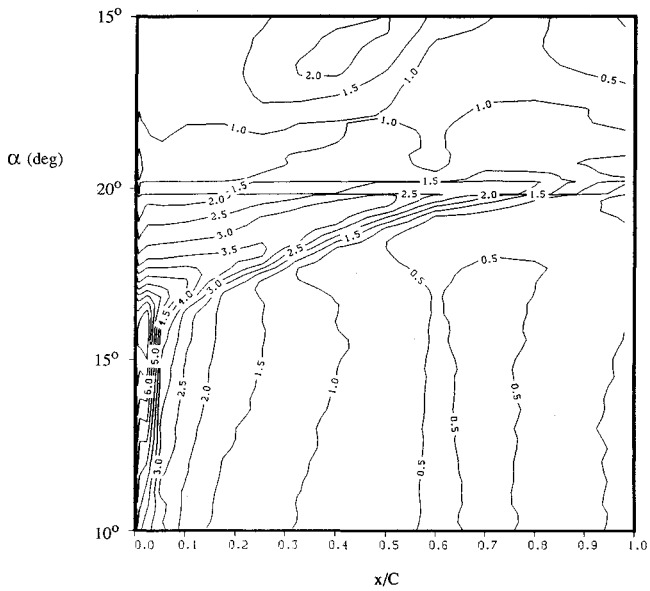

Fig. 4 Pressure coefficient contours for NACA 0012 at $M_\infty = 0.035$ and $k = 0.151$.

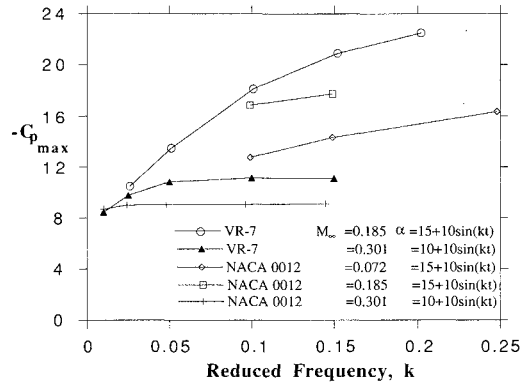

Fig. 5 Frequency effect for NACA 0012 and VR-7 airfoils.

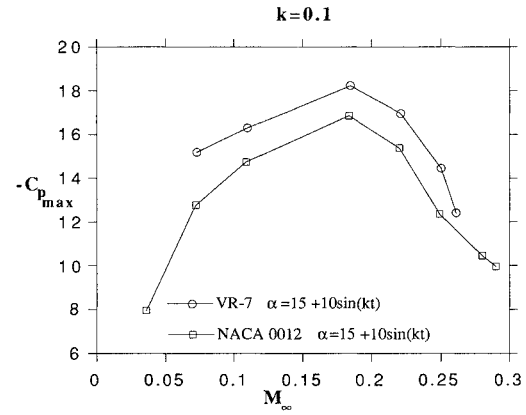

Fig. 6 Mach effect for NACA 0012 and VR-7 airfoils.

The effect of unsteadiness on the maximum suction peak, and hence the onset of stall, was examined using five cases (for two airfoils) from Ref. 6 carefully chosen to isolate unsteadiness from other effects. Figure 5 shows that the two airfoils respond differently to increasing frequency. Of particular interest is the slope, which characterizes the degree to which the onset of stall can be delayed by sinusoidal pitching with increasing frequency. For the higher Mach number the maximum suction peaks of both airfoils are relatively independent of frequency, whereas for the lower Mach number the maximum suction peak of the VR-7 increases much faster with increasing frequency than the NACA 0012. The dramatic differences among these slopes provided much of the impetus to concentrate on these two airfoils.

The effect of M_∞ on stall onset is investigated by comparing the same pitching motion for two different airfoils. Figure 6 shows how the maximum suction peak varies with Mach number. The results in Fig. 6 for different airfoils are simply offset by a constant. Both exhibit a slope change when the flow becomes Mach supercritical.

Boundary-Layer Analysis

It is evident that a better understanding is needed of the boundary layer before the onset of stall. Of particular interest is the region where the onset of stall begins near the leading edge. Since there are only two or three transducers in the first 2 or 3% of the chord, the experimental resolution near the leading edge is insufficient for a detailed characterization of the boundary layer. Thus, a computational approach was adopted, and a sequence of numerical calculations was performed. The implicit finite difference code ARC2D of Pulliam[10] was used to simulate the experimental results by solving the steady two-dimensional Euler equations over the range of α up to stall onset.

The NACA 0012 and the VR-7 were chosen from the eight airfoils tested in Ref. 6 because of their distinctive dynamic

stall behaviors. The Mach numbers 0.185 and 0.301 were chosen because most of the test cases were performed at these values. The angle of attack α was chosen to range from 7 deg to the point at which the steady calculation failed to converge because of shock-induced unsteadiness. Samples of computed results are summarized in Table 1. A typical computed pressure distribution is compared with the measured values for the same integrated lift C_ℓ in Fig. 7. For both airfoils and Mach numbers, at the same C_ℓ, surprisingly good agreement is found between the experimental pressure distributions and those computed on the basis of steady inviscid flow, up to the value of α at which the maximum suction peak or onset of stall occurs. Before stall onset, the lift slopes C_{ℓ_α} for the range of frequencies considered here are roughly parallel to and deviate by offsets of no more than and usually much less than half of a degree lag from that of the static stall. This suggests that, for the frequency range considered here (k less than 0.25 based on half chord), the attached flow before stall onset is quasisteady and viscous effects are unimportant to the pressure distribution. The computed pressure distributions were then used to estimate the growth of the boundary layer.

Separation refers to a condition such that the vorticity is no longer confined to the otherwise thin boundary layer. In two dimensions, the necessary condition for steady or unsteady separation is the existence of a line (lines) of zero vorticity ($\partial u/\partial y = 0$ for a boundary layer), dividing a small region of vorticity of one sign from the main vorticity field of the opposite sign. This line first appears with upstream and downstream ends on the surface, where the pressure gradient is sufficiently adverse. As α increases, the finite region adjacent to the airfoil and bounded by the zero vorticity line expands and moves toward the outer edge of the boundary layer. This thickening is followed by the zero vorticity line finally separating the boundary layer, unless a change of pressure gradient downstream draws the vorticity back to the wall or mixing is strong enough that the vorticity flux from the wall is neutralized (at least in a Reynolds-averaged sense) by the vorticity convected from upstream. A local saddle may appear along this line as the flow evolves, causing an abrupt thickening of the boundary layer and ejection of the retarded fluid, as depicted by Moore,[11] Rott,[12] and Sears and Telionis[13] (the MRS condition). A line of zero vorticity near a wall forms a local recirculating flow commonly referred to as a separation bubble. It is found that this definition of a separation bubble is suitable for the present analysis regardless of whether the initial separation is laminar, static, or dynamic. Thus, unconfined outward motion of the zero vorticity line will result in bubble bursting, boundary-layer separation, and the onset of

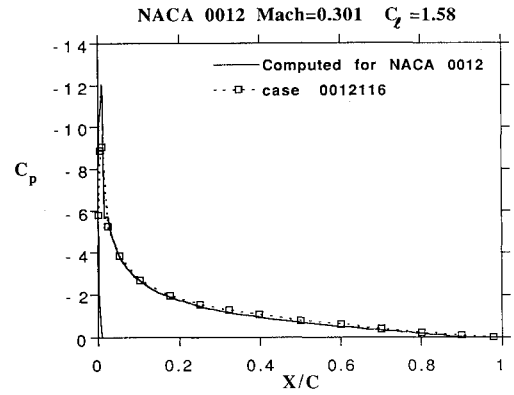

Fig. 7 Experimental and computed pressures at $M_\infty = 0.301$ for NACA 0012.

Table 1 Inviscid numerical results

Angle	Iterations	C_ℓ	C_D	C_m	Resid.	S-S Pts[b]
NACA 0012 low Mach number (0.185)						
7.0	2500	0.85117	0.00153	−0.00572	0.312E-10	0
9.0	3725	1.09231	0.00260	−0.00693	0.969E-14	0
11.0	4000	1.33199	0.00387	−0.00781	0.889E-14	0
13.0	4100	1.56987	0.00566	−0.00832	0.971E-14	0
15.0	4250	1.80547[a]	0.00774	−0.00836	0.845E-14	0
17.0	4400	2.03800[a]	0.01028	−0.00780	0.868E-14	0
19.0	4600	2.26577[a]	0.01348	−0.00645	0.860E-14	7
21.0	4300	2.47630[a]	0.01866	−0.00307	0.808E-14	24
NACA 0012 high Mach number (0.301)						
7.0	2575	0.87859	0.00206	−0.00495	0.805E-14	0
8.0	2675	1.00367	0.00277	−0.00512	0.972E-14	0
9.0	2675	1.12854	0.00360	−0.00505	0.364E-13	0
10.0	2950	1.25312	0.00458	−0.00496	0.762E-14	0
11.0	3000	1.37712[a]	0.00653	−0.00393	0.806E-14	13
12.0	2800	1.49765[a]	0.00767	−0.00241	0.872E-14	31
13.0	4800	1.57967[a]	0.01333	+0.00382	0.146E-13	49
VR-7 low Mach number (0.185)						
7.0	3500	0.94468	0.00176	−0.00488	0.210E-11	0
9.0	4000	1.18358	0.00294	−0.00691	0.182E-10	0
11.0	5000	1.42074	0.00447	−0.00881	0.474E-11	0
13.0	5000	1.65558[a]	0.00644	−0.01047	0.302E-12	0
15.0	5200	1.88732[a]	0.00894	−0.01182	0.839E-14	0
17.0	4450	2.11433[a]	0.01221	−0.01273	0.950E-14	0
19.0	4600	2.33228[a]	0.01670	−0.01287	0.913E-14	4
21.0	6000	2.50615[a]	0.02407	−0.00961	0.175E-12	15
VR-7 high Mach number (0.301)						
7.0	2675	0.97571	0.00232	−0.00451	0.881E-14	0
8.0	3300	1.09973	0.00305	−0.00520	0.926E-14	0
9.0	3825	1.22351	0.00390	−0.00573	0.941E-14	0
10.0	4200	1.34697	0.00490	−0.00606	0.968E-14	0
11.0	4300	1.46995	0.00609	−0.00615	0.841E-14	0
12.0	4300	1.59214[a]	0.00754	−0.00590	0.856E-14	3
13.0	4500	1.71225[a]	0.00944	−0.00517	0.654E-14	18
14.0	3100	1.81489[a]	0.01358	−0.00283	0.881E-14	37

[a]Denotes lift greater than static stall value. [b]Number of grid points at which flow is supersonic.

stall. For steady separation, the upstream end of this line, defined here as the initial separation point, coincides with the bifurcating streamline at the wall and extends out into the flow. The other end approaches infinity downstream or is fixed at the reattachment point if conditions allow.

A separating boundary layer will not reattach to form a short bubble unless the Reynolds number is high enough for the flow to become turbulent and mixing is strong enough to counteract the adverse pressure gradient. Tani[14] and Owen and Klanfer[15] independently proposed that bubbles be classified as short or long according to whether the Reynolds number at initial separation (R_{δ_s}) based on the displacement thickness exceeds a critical value of about 500. From his analysis of a collection of experimental results, Crabtree[16] concluded that bubble breakdown occurs when the pressure recovery coefficient σ, defined as the difference in pressure at reattachment and at initial separation, normalized by the dynamic pressure at separation, exceeds 0.35. In his review article, Tani[17] offered a unified view for bubble bursting as a failure of reattachment due to insufficient mixing, when either Re is below the transition value or the maximum possible shear stress set up in the turbulent flow is not strong enough to counteract the increasingly more adverse pressure gradient as α increases. Gaster[18] correlated the nondimensional pressure gradient parameter $\Lambda = (\theta_s^2/\nu)(\Delta U/\Delta S)$ with the momentum thickness R_{θ_s} at separation for bubbles measured in his experiments, as well as in those of McGregor[19] and Crabtree.[20] He found that, when characterized by the two parameters Λ and R_{θ_s}, short bubbles burst to form long ones as the inclined straight line in the Λ-R_{θ_s} plane (Fig. 8) is crossed. The symbols on the same figure indicate the cases computed here, all but one of which are in the short bubble region. The ones closer to the inclined straight line correspond to higher α, and the closest ones correspond to flows with a local supersonic region. A reduction in Re will shift these values toward both the bursting criteria of Owen and Klanfer (shown as the vertical line in Fig. 8) and Gaster, a trend consistent with the earlier observation that static stalls on the NACA 0012 at the lowest Reynolds number ($M_\infty = 0.035$) differ from those at higher Reynolds numbers. It is interesting to note that most of these values are below $R_{\theta_s} = 350$, a value below which Evans and Mort[21] attributed static stall to bubble bursting and above which static stall was ascribed to turbulent reseparation.

To study bubble bursting mechanisms, Curle and Skan[22] used the normalized displacement thickness K, the ratio of the Reynolds number at separation to the square root of the freestream Reynolds number. The value of K can be calculated by integrating the computed inviscid pressure distribution (or the velocity U at the outer edge of the boundary layer) from the stagnation point to the assumed separation point S', where U has fallen 6% from its maximum value, viz.,

$$K = \frac{3.7U_{S'}}{U_\infty}\sqrt{0.441\left(\frac{U}{U_\infty}\right)^{-6}\int_0^{S'}\left(\frac{U}{U_\infty}\right)^5 \mathrm{d}\left(\frac{S'}{c}\right)} \qquad (1)$$

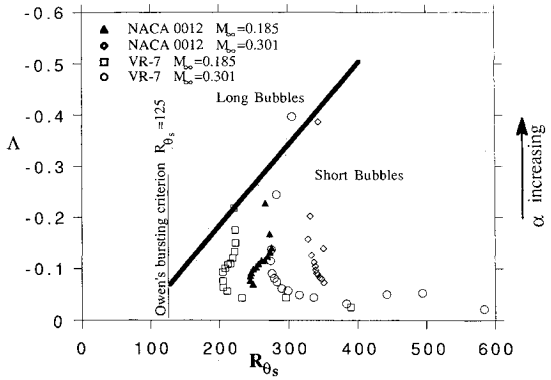

Fig. 8 Gaster's criterion for long and short bubbles.

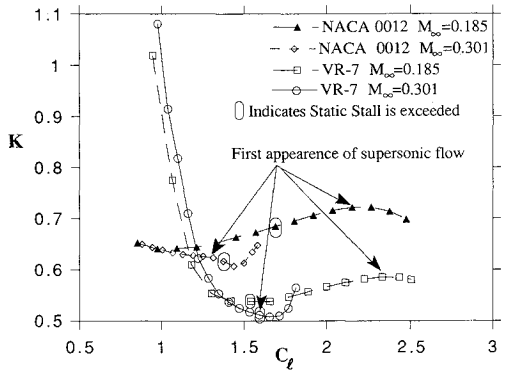

Fig. 9 Curle and Scan's bubble bursting criterion.

They observed that K drops fairly sharply to a minimum as C_ℓ or α increases. They thus proposed that, if K is so large that R_{δ_s} exceeds 500 (125 for R_{θ_s}), immediate reattachment is favorable and the separation bubble will be short, whereas if K falls below the critical value before the minimum, bubble bursting may occur. They further proposed that if the minimum has passed and bursting has not occurred, a further increase in C_ℓ will not cause the bubble to burst, since the flow would be increasingly turbulent.

Figure 9 shows the variation of K for the two airfoils and two Mach numbers. Before the flow becomes locally supersonic, indicated by the arrows, the curves for the higher value of M_∞ follow closely those for the lower value. This suggests that the growth of the boundary layer is largely unaffected by compressibility until the local flow reaches Mach-critical condition. Shortly before the flow becomes locally supersonic, both curves for the higher M_∞ further decrease to a minimum below the value for static stall, indicated by the oval symbols, whereas the curves for the lower M_∞ have begun to rise before the static stall value is reached. As α increases, the focusing tendency of a compression wave in supersonic flow causes the initial separation point to move upstream toward the stagnation point faster than in subsonic flow, resulting in the further decrease in K relative to the subsonic case. Although these K values were computed using the quasisteady assumption, they reflect the high tendency of the boundary layer to separate under a supersonic compression. Since for the lower Mach number, α at the first minimum is below the static stall value for both airfoils, bursting does not occur. If the bubble does not burst at or before the first minimum, bursting is unlikely to become the onset mechanism for static stall because the flow becomes increasingly turbulent as the lift increases. Therefore, static stall is of the trailing-edge type, which agrees with the data in Ref. 6 for both airfoils. The cause for the second descent is again the change from subsonic to locally supersonic flow, shown by arrows for each case. Hence, bubble bursting is likely to be the mechanism for the onset of static or dynamic stall, for flows that are Mach supercritical at the leading edge.

The difference between the K-C_ℓ plots for the two airfoils at lower lift values provides an explanation for the distinct stall onset characteristics discussed earlier with reference to Fig. 5. At lower C_ℓ values (or α) the drastic drop in K for the VR-7 indicates that the boundary layer is turbulent and susceptible to reattachment until the lift is close to the static stall value, whereas for the NACA 0012 K remains roughly constant and even slightly lower (more laminar) than the static stall value. Thus under dynamic conditions the separation process can begin earlier, which corresponds to a shorter stall onset delay for the NACA 0012 than for the VR-7.

For flows that are everywhere subsonic, bubble bursting must not be excluded from consideration as the onset mechanism for dynamic stall. The alternative, turbulent reseparation, advocated first by Wallis[23] and further supported by the

analysis of Evans and Mort[21] for static stall, is ambiguous and, as Tani[17] pointed out, amounts to bubble breakdown itself for the cases considered by Wallis. For the same dynamic stall data set considered here, McCroskey et al.[24] asserted, "In most cases, including the leading-edge stall on the basic NACA 0012 profile, dynamic stall was found *not* to originate with the bursting of a laminar separation bubble, as is commonly believed, but with a breakdown of the turbulent boundary layer." The basis for their assertion was the fact that abrupt flow reversal was detected in a region between 5 and 20% chord before a similar but less abrupt reversal was detected near the leading edge. On the contrary, the fact that most dynamic stall vortices first appear within 2% of the leading edge implies that the MRS separation condition was satisfied in that vicinity before the appearance or, equivalently, the existence of a zero vorticity line or separation bubble. It is well accepted that flow reversal may precede but does not necessarily imply separation. As α increases past static stall, the upstream end of the zero vorticity line moves approximately with the suction peak toward the stagnation point whereas the downstream end does not react as fast. This results in an elongated bubble, as noted by Johnson and Ham.[4] The onset point, as depicted by the MRS criterion and described as a fluid element being squashed into a protruding jet on both sides of a flow saddle,[25] would more likely be near the upstream end of the zero vorticity line near the leading edge, where the reverse flow is decelerated, than on the reattaching end or elsewhere downstream where the pressure gradient is less adverse and the turbulence intensity is higher. Although initiation of a second vortex is sometimes identifiable downstream, and the reverse flow at the trailing edge moves upstream as α increases, both events are weak and incapable of causing abrupt stalls.

Effect of Transition

Since bubble bursting or failure to reattach is likely to be the onset mechanism of leading edge stall, we conducted a numerical assessment of the effect of transition on reattachment using the Baldwin and Lomax[26] turbulence model, an option in ARC2D for steady viscous flow predictions. This model was chosen for its simplicity, popularity, and applicability for mildly separated flows. Like all other models known to us, it is not expected to give a faithful description of the flow once massive separation occurs. The focus here is to study the stability of the flow when it is still reasonably attached.

An algebraic turbulence model works in a code by addition of an eddy viscosity to the flow starting from a user-specified point along the streamwise coordinate. This point mimics, in some sense, the transition from laminar to turbulent flow and is critical to the calculation of lift values and the identification and classification of laminar separation bubbles. The location of the transition point at the leading edge corresponds to tripping the boundary layer at the leading edge in an experiment. Alternatively, if the transition point was too far downstream, laminar separation would occur with no immediate reattachment and the calculation might not approach a steady state. Table 2 lists a series of computational experiments conducted to study the effect of transition point placement on flow reattachment. (More details are given in Currier.[27])

For $M_\infty = 0.185$ and a moderate $\alpha = 10$ deg, the flow is relatively insensitive to transition point placement. With a point of transition (TP) from laminar to turbulent flow for the numerical model of 0.01 or 0.02 chord, the computed lift value rapidly reaches an asymptotic value and the root mean square residual averaged over the entire grid is low, suggesting a converged solution. When the TP is moved to 0.1, the

Table 2 Transition point study for NACA 0012

α	TP	Iterations	Residual	C_ℓ comp.	C_ℓ exper.	%error C_ℓ
$M_\infty = 0.185$, $Re = 2.37 \times 10^6$, $\alpha_{stall} = 15.93$ deg, $C_{\ell ss} = 1.59$						
10.00	0.0100	5000	0.183E-12	1.08408	1.08	0.38
10.00	0.0200	5000	0.183E-11	1.08800	1.08	0.74
10.00	0.1000	5000	0.610E-07	1.03494	1.08	4.17
10.00	0.5000	5000	0.265E-05	0.49959	1.08	53.7
13.25	0.0050	5000	0.693E-12	1.40177	1.38	1.58
13.25	0.0100	5000	0.403E-12	1.40763	1.38	2.00
13.25	0.0125	5000	0.840E-11	1.41054	1.38	2.21
13.25	0.0150	5000	0.408E-11	1.41064	1.38	2.22
13.25	0.0160	5000	0.534E-12	1.39451	1.38	1.05
13.50	0.0160	5000	0.323E-09	1.41439	1.39	2.44
14.00	0.0160	5000	0.685E-08	1.44385	1.43	0.96
14.50	0.0160	5000	0.594E-08	1.47493	1.46	1.02
15.00	0.0160	5000	0.651E-07	1.48368	1.49	0.42
15.00	0.0200	5000	0.165E-06	1.41001	1.49	5.37
15.50	0.0100	5000	0.110E-11	1.61433	1.52	6.21
15.50	0.0150	5000	0.160E-11	1.57660	1.52	3.72
15.50	0.0160	5000	0.108E-06	1.37093	1.52	9.81
15.50	0.0175	5000	0.108E-06	1.37093	1.52	9.81
15.50	0.0200	5000	0.955E-07	1.41203	1.52	7.10
15.50	0.0250	5000	0.138E-05	1.43104	1.52	5.85
$M_\infty = 0.301$, $Re = 3.37 \times 10^6$, $\alpha_{stall} = 13.43$ deg, $C_{\ell ss} = 1.371$						
10.00	0.0000	5000	0.498E-09	1.11637	1.11	0.57
10.00	0.0100	5000	0.643E-13	1.12422	1.11	1.28
10.00	0.0150	4500	0.643E-14	1.12675	1.11	1.51
10.00	0.0200	5000	0.816E-13	1.12779	1.11	2.53
13.25	0.0000	5000	0.647E-13	1.42638	1.37	4.12
13.25	0.0050	5000	0.103E-11	1.43844	1.37	5.00
13.25	0.0100	5000	0.265E-11	1.44003	1.37	5.11
13.25	0.0125	5000	0.115E-11	1.43179	1.37	4.51
13.25	0.0135	5500[a]	0.887E-07	1.43278	1.37	4.48
13.25	0.0135	6000[a]	0.249E-06	1.43454	1.37	4.71
13.25	0.0135	7000[a]	0.173E-05	1.43771	1.37	4.94

[a]Iterations beginning with 5001 are time accurate, not steady. These runs were started from the converged solution of the 5000 iteration for $\alpha = 13.25$ with a transition point of 0.0125.

residual reflects a solution that is not converged, but the lift value is still reasonable. If the TP is moved to 0.5, the flow becomes massively separated. These results show that without the eddy viscosity, massive separation would occur long before the static stall angle. However, with a downstream turbulent flow starting at 10% chord, the boundary layer is only marginally unstable. The sensitivity to transition point placement near stall increases significantly. When α is increased to 15.5 deg (0.4 deg below the static stall angle), fully converged solutions with reasonable lift values were obtained for transition points of 0.01 and 0.015. However, if the transition point is moved to 0.016, the flow becomes intermittently separated. Moving the transition point from 0.015 to 0.016 corresponds to moving the TP one grid line. This shows that the flow near stall is sensitive to changes in transition location of 0.1% chord.

To examine the effects of Mach-supercritical flow on transition point sensitivity, several computations were made for $M_\infty = 0.301$, including some at the moderate α of 10 deg for which the results behaved like the $M_\infty = 0.185$ cases. For $\alpha = 13.25$ deg (slightly below the static stall value 13.43 deg) and transition points up to 0.0125, reasonably accurate lift values with well-converged solutions were obtained, as shown in Table 2. The Mach contours and local flow vectors are shown in Fig. 10 for the transition point set at 0.0125, marked by the triangle. The darker contour outlines the sonic bubble in which the flow is supersonic. When the transition point was moved to 0.0135, again down one grid line and 0.1% chord, the calculation produces negative densities during the computation unless time-accurate marching with a small enough time step is used. Subsequent to moving the transition point, the flow develops rapidly. After 500 time steps, which corresponds to the flow traveling one-half chord from the time the transition point is moved, the sonic line on the downstream side, or shock, has deformed and moved almost one grid line downstream toward the transition point, even though the lift value has not changed significantly. After 2000 time steps, Fig. 11 shows that a separation much more massive than at the lower M_∞ has occurred, leading later to a sudden drop in C_l. This numerical experiment shows that a locally supersonic flow interacts more strongly with the boundary layer and is more sensitive to transition than the previous Mach-subcritical flow.

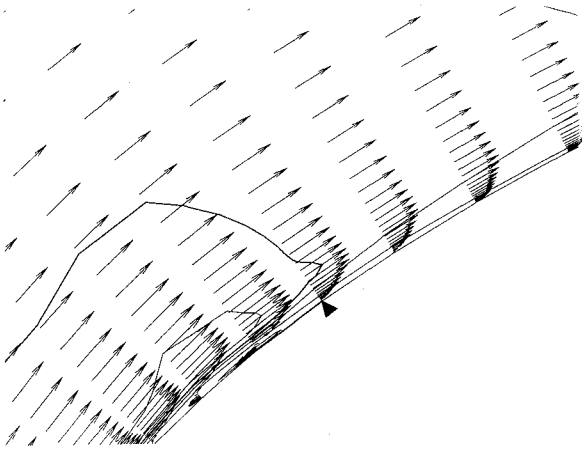

Fig. 10 Navier-Stokes solution for $M_\infty = 0.301$, $\alpha = 13.25$ deg, TP = 0.0125, and iterations = 5000.

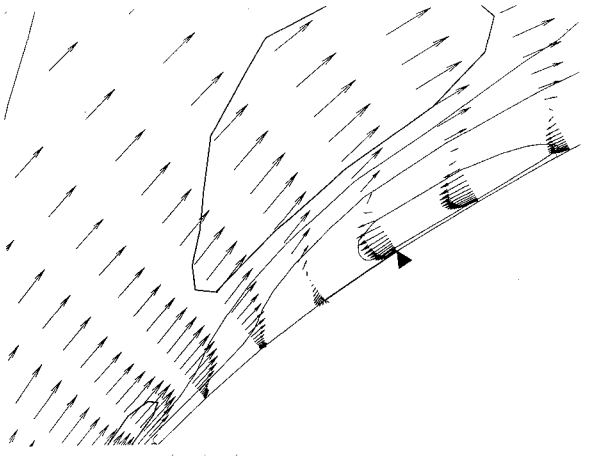

Fig. 11 Navier-Stokes solution for $M_\infty = 0.301$, $\alpha = 13.25$ deg, TP = 0.0125, time steps = 2000, from the solution on Fig. 10.

The difficulty of predicting transition for realistic flows and the overly simplified turbulence model used for separating flows cast doubts on the validity of these numerical experiments. However, they do show that the mean flow is marginally stable at angles of attack near stall and is very sensitive to small changes in the boundary layer. As reported by Johnson and Ham,[4] the initial (laminar) separation point of the separation bubble moves almost instantaneously toward the stagnation point, whereas the upstream movement of the reattachment point is delayed as much as the onset of stall. It is conceivable that, as α approaches the static stall angle, the upstream end of the zero vorticity line and hence the initial separation region move toward the stagnation point as fast as the suction peak and experience an environment less favorable for the occurrence of transition. Since the reattachment point does not move upstream as fast as the initial separation point, transition is delayed to a location further downstream relative to the initial separation point. Without the benefit of transition, the growth of the zero vorticity line, or the separation bubble, becomes unbounded and the onset of stall becomes imminent. When the flow becomes supersonic at the leading edge, the steepening compression moves the upstream part of the zero vorticity line closer to the stagnation point than in a subsonic flow, as indicated by the drop in K. As a result, transition is further delayed, thus making the flow even more globally unstable.

Effect of Unsteadiness on Stall Onset

Since Prandtl's time, theories of separation have been built largely on the boundary-layer equation. The concept of separation, as Prandtl introduced it, is akin to the concept of a thin vortical layer confined to the surface of a body in an otherwise irrotational flow. Therefore, it is natural to associate the failures of the boundary-layer equation with separation, especially when most observable breakdowns of the boundary layer are catastrophic. Indeed, since a laminar flow can only support a weak adverse pressure gradient without separation, and the separating free shear layer is highly unstable, it is quite reasonable to conjecture that the breakdown occurs soon after the boundary-layer equation fails to be analytic, or to assume that the breakaway time is so short compared with other characteristic times of the flow that for practical purposes, such as stall prediction, it is instantaneous.

The dynamic effects on the delay of stall have been perceived as favorable because of the delay of separation, which would otherwise be catastrophic. So far, all observations indicate that, at least for Mach-subcritical flows, the onset of stall on an upward pitching airfoil is delayed to an angle beyond the static stall angle, and this is readily attributable to the delay of separation. However, after substantial effort, we concluded that no significant effect of unsteadiness other than the stall delay can be documented. As mentioned earlier, for the range of reduced frequencies considered, the lift slopes before stall onset deviate little from the static lift slope. This means that, as far as the growth of the boundary layer is concerned, the local acceleration $\partial u_e/\partial t$ (proportional to the product of the lift slope, theoretically 2π, and the pitch rate) is only of order of $2\pi\alpha_1 k$, which is much less than the deceler-

ation effect due to the adverse pressure gradient. For a pitching amplitude of $\alpha_1 = 10$ deg and a reduced frequency of $k = 0.2$, each one-degree change in incidence corresponds to downstream movement of a fluid element by $\pi/(4\alpha_1 k)$ or 40% chord. The thickness δ of the boundary layer at a given location x is proportional to $x/\sqrt{Re_x}$. Hence, a characteristic viscous time for the boundary layer at x to react to a change of outer flow pressure is $\delta^2/\nu = x/U$. At the leading edge, where x is measured by the leading edge radius of curvature, the time for the boundary layer to catch up corresponds to only a fraction of a degree change in incidence. Even for the entire boundary layer, at the trailing edge $x = 1$, the lag that corresponds to one chord length traveled is only 2.5 deg using the most conservative estimate, whereas the outer flow is already within one-half degree of the corresponding static flow. In other words, the boundary layer at the leading edge retains very little of its history. Therefore, it is well justified to take the flow at the leading edge to be quasisteady until the separation process begins. Moreover, the incidence angle is not a good indicator of events occurring in the boundary layer.

When the onset time t_{onset} is measured (using the dimensionless time to travel one-half chord rather than using α) from the time the airfoil passed the static stall angle t_s, a different picture emerges. Figure 12 shows onset delays $\Delta T_s = t_{\text{onset}} - t_s$ computed for sinusoidal oscillations, i.e., $\alpha(t) = \alpha_0 + \alpha_1 \sin(kt)$, as

$$\Delta T_s = \frac{1}{k}\left[\sin^{-1}\left(\frac{\alpha_{C_{p_m}} - \alpha_0}{\alpha_1}\right) - \sin^{-1}\left(\frac{\alpha_s - \alpha_0}{\alpha_1}\right)\right] \qquad (2)$$

and for pitch ramps, $\alpha(t) = \alpha_0 + At$, as $(\alpha_{C_{p_m}} - \alpha_s)/A$, where $\alpha_{C_{p_m}}$, α_s, α_0, and α_1 are the angle at maximum suction peak, the static stall angle, and the mean and amplitude of oscillation, respectively, and A is the dimensionless pitch rate in degrees per half-chord traveled. Except for two values for the VR-7 at the lowest reduced frequencies 0.01 and 0.026, all onset delays decrease monotonically with reduced frequency (or dimensionless pitch rate in radians). In other words, the onset of stall occurs sooner rather than later as the pitch rate increases; increased unsteadiness speeds up the separation process rather than delaying it. The Mach number for the VR-7 and NACA 0012 (McCroskey et al.) cases is 0.185 and for the SSC-A09 (Lorber and Carta) is 0.2. Table 3 lists the data used for computing the delays on the NACA 0012. The cases for the lowest reduced frequency were considered quasisteady and used as the reference for time delay computations. It is important to note that the choice of the reference time at which the airfoil passes a fixed angle does not affect the frequency dependence of the onset delay. A different choice simply shifts all of the values up or down except for values at the lowest reduced frequency. Nonetheless, the reason for this choice is

Table 3 Onset delays on NACA 0012

Remarks	Case no.	M_∞	k	α_0	α_1	$\alpha_{C_{p_m}}$	ΔT_s
	8306	0.184	0.0990	15.00	14.00	23.571	5.759
	8220	0.184	0.0990	15.00	10.00	22.333	7.058
	8222	0.184	0.1490	15.00	10.00	23.158	5.569
Trip	14,019	0.183	0.0500	15.00	10.00	17.742	5.383
Trip	14,104	0.183	0.0500	15.00	10.00	17.783	5.468
Trip	14,106	0.184	0.0990	15.00	10.00	18.615	3.649
Trip	14,021	0.182	0.1000	15.00	10.00	18.625	3.623
Trip	14,108	0.183	0.1490	15.00	10.00	19.483	3.062
Trip	14,023	0.182	0.1500	15.00	10.00	19.475	3.036
	9022	0.184	0.2350	15.00	6.00	20.907	5.047
	9101	0.184	0.2840	15.00	5.00	19.805	3.663
	9106	0.184	0.2450	10.00	10.00	19.491	2.353
	9110	0.184	0.0100	8.00	10.00	17.007	15.286
	9112	0.183	0.0500	8.00	10.00	17.855	8.635
	9118	0.184	0.1990	8.00	10.00	17.718	1.830
	12,310	0.186	0.0010	7.00	10.00	16.240	0.000
Trip	13,313	0.181	0.0010	7.00	10.00	15.086	0.000

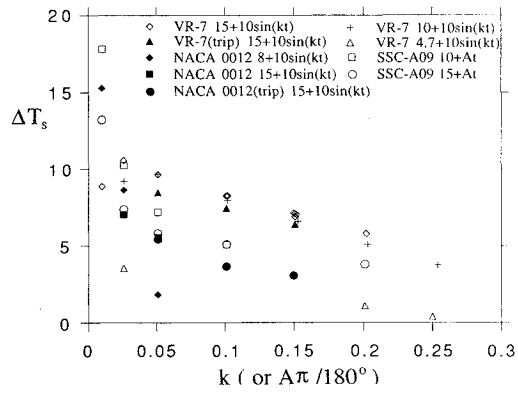

Fig. 12 Effect of unsteadiness on dynamic stall onset delay time from static stall for different airfoils undergoing different pitching motions.

clear. Since upward pitching at higher frequency delays to higher α the adverse pressure gradient that the boundary layer would experience at static stall, the process of separation for all frequencies is not likely to begin before the static stall angle is reached. This assumption is substantiated by the fact, mentioned earlier, that all suction peak values corresponding to a stall for nonzero pitching frequencies are at or above the static stall values. It should also be noted that all cases shown here were chosen so that the stall onset occurs before the maximum angle is reached. Placing a trip at the leading edge does not change the onset delay characteristics. The minor differences are attributable to the choice and uncertainty of the static stall angle. For all cases, again excepting the VR-7, the trends at lower frequencies suggest that completion of the separation process takes a finite time, comparable to other time scales of the flow, before its effects can be felt or measured in a global sense.

Based on computations using a Lagrangian form of the boundary-layer equation, Shen and Wu[28] found that the separation time for flow over a cylinder is systematically delayed by deceleration and advanced by acceleration and remarked that their finding was contrary to expectations. The results shown here seem to support their conclusion. If so, the advantage of dynamic stall is simply to move fast enough so that onset occurs at a higher angle and to maintain high lift by keeping the dynamic stall vortex on the surface.

Conclusions

The results of this study clarify, support, and extend the analysis and observations reported in Fung and Carr[9] showing that the onset of dynamic stall depends on whether the flow is Mach subcritical or supercritical. In addition, it is found that, although the dependence of the onset on M_∞ is the same for different airfoils, the dependence on frequency can be very different for different airfoils, or for airfoils with differently shaped leading edges, and that the flow before stall onset is predictable on a quasisteady basis by inviscid theory.

Following the classification of static stalls by a Reynolds number typical of the local condition of separation rather than using the Reynolds number based on the chord, the present analysis shows that most dynamic stall cases studied here belong to the range of Reynolds number for which stall onset is ascribed to bursting of the separation bubble, arising from failure of the boundary layer to reattach. It also suggests that bursting is promoted by the focusing compression that shifts the bubble to a more laminar environment when the outer flow becomes locally supersonic. Numerical study of the sensitivity of stall onset to transition location further supports the identification of bubble bursting due to delay in transition as the mechanism of stall onset.

Lastly, our analysis suggests that completion of the process of separation requires a finite time comparable to other time

scales for the flow and that, although increased unsteadiness delays the occurrence of the onset to a higher angle, it actually promotes the process of boundary-layer separation.

Acknowledgments

This research has been supported by Air Force Office of Scientific Research Grant 88-0163 monitored by Hank Helin and by a Cooperative Research Grant between the Institute of Astronautics and Aeronautics of the National Cheng-Kung University, Republic of China, and the Computational Fluid Mechanics Laboratory of the University of Arizona. The computer support of NASA Ames Research Center for this and other related research is gratefully acknowledged. The authors would like to thank Lawrence Carr and Peter Lorber for providing the data sets.

References

[1]McCullough, G. B., and Gault, D. E., "Examples of Three Representative Types of Airfoil-Section Stall at Low Speed," NACA TN 2502, Sept. 1951.

[2]Ham, N. D., and Garelick, M. S., "Dynamic Stall Considerations in Helicopter Rotors," *Journal of the American Helicopter Society,* Vol. 13, No. 2, 1968, pp. 49–55.

[3]Harper, P. W., and Flanigan, R. E., "The Effect of Change of Angle of Attack on the Maximum Lift of a Small Model," NACA TN 2061, March 1950.

[4]Johnson, W., and Ham, N. D., "On the Mechanism of Dynamic Stall," *Journal of the American Helicopter Society,* Vol. 17, No. 4, 1972, pp. 36–45.

[5]Ericsson L. E., and Reding, J. P., "Fluid Mechanics of Dynamic Stall, Part I: Unsteady Flow Concepts," *Journal of Fluids and Structures,* Vol. 2, No. 1, 1988, pp. 1–33.

[6]McCroskey, W. J., McAlister, K. W., Carr, L. W., and Pucci, S. L., "Experimental Study of Dynamic Stall on Advanced Airfoil Sections," NASA TM-84245, Vols. I–III, Sept. 1982.

[7]Lorber, P. F., and Carta, F. O., "Unsteady Stall Penetration Experiments at High Reynolds Number," Air Force Office of Scientific Research, AFOSR TR-87-1202, Bolling AFB, Washington, DC, April 14, 1987.

[8]Rhode R. S., "Correlation of Flight Data on Limit Pressure Coefficients and Their Relation to High-Speed Burbling and Critical Tail Loads," NACA ACR No. I4I27, Sept. 1944.

[9]Fung, K.-Y., and Carr, L. W., "The Effects of Compressibility on Dynamic Stall," *AIAA Journal,* Vol. 29, No. 2, 1991, pp. 306–308.

[10]Pulliam, T., "Euler and Thin Layer Navier Stokes Codes: ARC2D, ARC3D, Notes for Computational Fluid Dynamics User's Workshop," Univ. of Tennessee Space Inst., Tullahoma, TN, March 12–16, 1984.

[11]Moore, F. K., "On the Separation of the Unsteady Laminar Boundary Layer," *Boundary Layer Research,* edited by H. G. Goertler, Springer-Verlag, Berlin, 1958, pp. 296–311.

[12]Rott, N., "Unsteady Viscous Flows in the Vicinity of a Separation Point," *Q. Appl. Math.,* Vol. 13, No. 4, 1956, pp. 444–451.

[13]Sears, W. R., and Telionis, D. P., "Unsteady Boundary-Layer Separation," *Fluid Dynamics of Unsteady, Three-Dimensional and Separated Flows,* Proceedings of the June 1971 SQUID Workshop, Purdue Univ., West Lafayette, IN, 1971, pp. 446–466.

[14]Tani, I., "Note on the Interplay Between the Laminar Separation and the Transition from Laminar to Turbulent of the Boundary Layer," *Journal of the Society of Aeronautical Sciences of Japan,* Vol. 6, Feb. 1939, pp. 122–134.

[15]Owen, P. R., and Klanfer, L., "On the Laminar Boundary Layer Separation from the Leading Edge of a Thin Aerofoil," British Aeronautical Research Council, RAE Rept. Aero. 2508 (Oct. 1953); reissued as ARC Current Paper No. 220, Farnborough, England, UK, 1955.

[16]Crabtree, L. F., "The Formation of Regions of Separated Flow on Wing Surfaces, Part II: Laminar-Separation Bubbles and the Mechanism of the Leading-Edge Stall," Royal Aircraft Establishment, RAE Rept. Aero. 2528, July 1954; reissued as ARC R&M 3122, Farnborough, England, UK, 1959.

[17]Tani, I., "Low-Speed Flows Involving Bubble Separations," *Progress in Aeronautical Sciences,* Vol. 5, Pergamon Press, New York, 1964, pp. 70–103.

[18]Gaster, M., "The Structure and Behavior of Laminar Separation Bubbles," AGARD Conference Proceedings 4, 1966, pp. 819–854.

[19]McGregor, I., "Regions of Localized Boundary Layer Separation and Their Role in the Nose-Stalling of Aerofoils," Ph.D. Thesis, Queen Mary College, Univ. of London, 1954.

[20]Crabtree, L. F., "Effects of Leading-Edge Separation on Thin Wings in Two-Dimensional Incompressible Flow," *Journal of the Aeronautical Sciences,* Vol. 24, No. 8, 1957, pp. 597–604.

[21]Evans, W. T., and Mort, K. W., "Analysis of Flow Parameters for a Set of Sudden Stalls in Low-Speed Two-Dimensional Flow," NASA TN D-85, Aug. 1959.

[22]Curle, N., and Skan, S. W., "Calculated Leading-Edge Laminar Separations from Some RAE Aerofoils," British Aeronautical Research Council, ARC CP 504, 1960.

[23]Wallis, R. A., "Boundary Layer Transition at the Leading Edge of Thin Wings and Its Effect on General Nose Separation," *Advances in Aeronautical Sciences,* Vol. 3, Pergamon Press, New York, 1962, pp. 161–184.

[24]McCroskey, W. J., Carr, L. W., and McAlister, K. W., "Dynamic Stall Experiments on Oscillating Airfoils," *AIAA Journal,* Vol. 14, No. 1, 1976, pp. 57–63.

[25]Van Dommelen, L. L., and Shen, S. F., "The Spontaneous Generation of the Singularity in a Separating Laminar Boundary Layer," *Journal of Computational Physics,* Vol. 38, No. 2, pp. 125–140.

[26]Baldwin, B. S., and Lomax, H., "Thin Layer Approximation and Algebraic Model for Separated Turbulent Flows," AIAA Paper 78-257, Jan. 1978.

[27]Currier, J. M., "Investigation of Dynamic Stall Mechanisms on Airfoils," Masters Thesis, Univ. of Arizona, Tucson, AZ, May, 1990.

[28]Shen, S. F., and Wu, T., "Unsteady Separation over Maneuvering Bodies," AIAA Paper 88-3542-CP, Pt. 2, 1st National Fluid Dynamics Congress, Cincinnati, OH, July 25–28, 1988.